



## Geochemistry and background concentration of major ions in spring waters in a high-mountain area of the Hamedan (Iran)



Mohsen Jalali \*, Mahdi Jalali

Department of Soil Science, College of Agriculture, Hamadan, Iran

### ARTICLE INFO

#### Article history:

Received 14 July 2015

Revised 4 January 2016

Accepted 14 February 2016

Available online 20 February 2016

#### Keywords:

Chemical composition

Spring water

Hydrochemistry

Principal component

### ABSTRACT

Little is known about the natural phenomena that govern the chemical composition of spring waters in Alvand mountain ecosystem. A total of 50 spring water samples of the Alvand mountains, Hamadan, western Iran were collected and analyzed for the main components in an effort to both identify ion chemistry and establish background concentrations of major ions and some trace elements (Cd, Fe, Mn, Ni, Zn). The order of relative abundance of major cations in the spring waters was Ca, Mg, Na, K, while that of anions was  $\text{HCO}_3^-$ , Cl,  $\text{SO}_4^{2-}$ ,  $\text{NO}_3^-$ . Most spring water samples were undersaturated with respect to calcite. The major water types in spring waters were Ca– $\text{HCO}_3^-$  (group 1), Ca $\text{HCO}_3^-$ –Cl, CaMg– $\text{HCO}_3^-$ Cl, and CaMg–Cl– $\text{HCO}_3^-$  (group 2), which were mainly due to the dissolution of carbonate minerals and silicate weathering and partly due to the ion exchange. Activity diagrams showed that spring waters fall into the kaolinite field due to the short interaction with silicate minerals. In general, mineralization, pH, mean concentrations of Ca, Mg,  $\text{HCO}_3^-$ , TDS, saturation indices of calcite, dolomite and  $\text{PCO}_2$  were greater in water samples from the group 1 than in water samples from group 2. Spring waters were mainly soft water (84%) in group 2 and hard water (16%) in group 1. The factor analysis performed on spring water samples identified four factors controlling their variability in spring water samples. Four extracted factors explained 84.7% of data set variance. Factor 1 had the highest factor loadings of EC,  $\text{HCO}_3^-$ ,  $\text{SO}_4^{2-}$ , Cl, Ca, Mg, Na, Mn, Cd, Ni, and Fe, while factor 2 had the highest factor loadings of Zn. Factors 3 and 4 had the highest factor loading for  $\text{NO}_3^-$ , P and K, respectively. Factors 1, 2 and 4 together may be related to the dissolution of carbonate minerals (group 1) and silicate weathering, while factor 3 may be due to the anthropogenic input. Different statistical methods were used in the evaluation of background values of the spring waters. Trace element concentration in spring waters was low and associated with local mineralogy.

© 2016 Elsevier B.V. All rights reserved.

### 1. Introduction

Spring waters in Alvand mountain are the most important natural resources in Hamedan, western Iran and function as drinking water supply in regions, meanwhile, they are also used for agriculture irrigation. The spring waters of Alvand mountain areas are generally characterized by relatively low mineralization. Waters from high mountain basins have high quality and can be used as models of natural basin functioning (Zelazny et al., 2011). A detailed and thorough understanding of geochemical processes that control primarily chemical composition of water in high mountain springs is needed to improve understanding of biogeochemical cycles and better management of water resources in such ecosystem

(Zelazny et al., 2011). The chemical composition of spring waters in mountain basins is determined by rainfall, interaction of the precipitation with the surrounding rocks, soils, land vegetation and land use in the catchment areas (Allan and Flecker, 1993). To study and evaluate pollution of surface and groundwater, knowledge of natural background concentrations of ions and trace elements is required and their concentrations can be originated both by natural weathering and anthropogenic activities (Margiotta et al., 2012).

While much research has been done on the geochemical characteristics of springs by a number of researchers (e.g. Marini et al., 2000; Grasby and Hutcheon, 2000; Ragno et al., 2007; Lourenço et al., 2010; Zelazny et al., 2011; Zhang et al., 2011; Margiotta et al., 2012; Bozau et al., 2013; Nisi et al., 2013; Bottoni et al., 2013; Boy-Roura et al., 2013; Matić et al., 2013; Miller et al., 2015), limited information is available on the geochemistry of spring waters in a high-mountain area of Iran (Karimi et al., 2005).

\* Corresponding author.

E-mail address: [Jalali@basu.ac.ir](mailto:Jalali@basu.ac.ir) (M. Jalali).

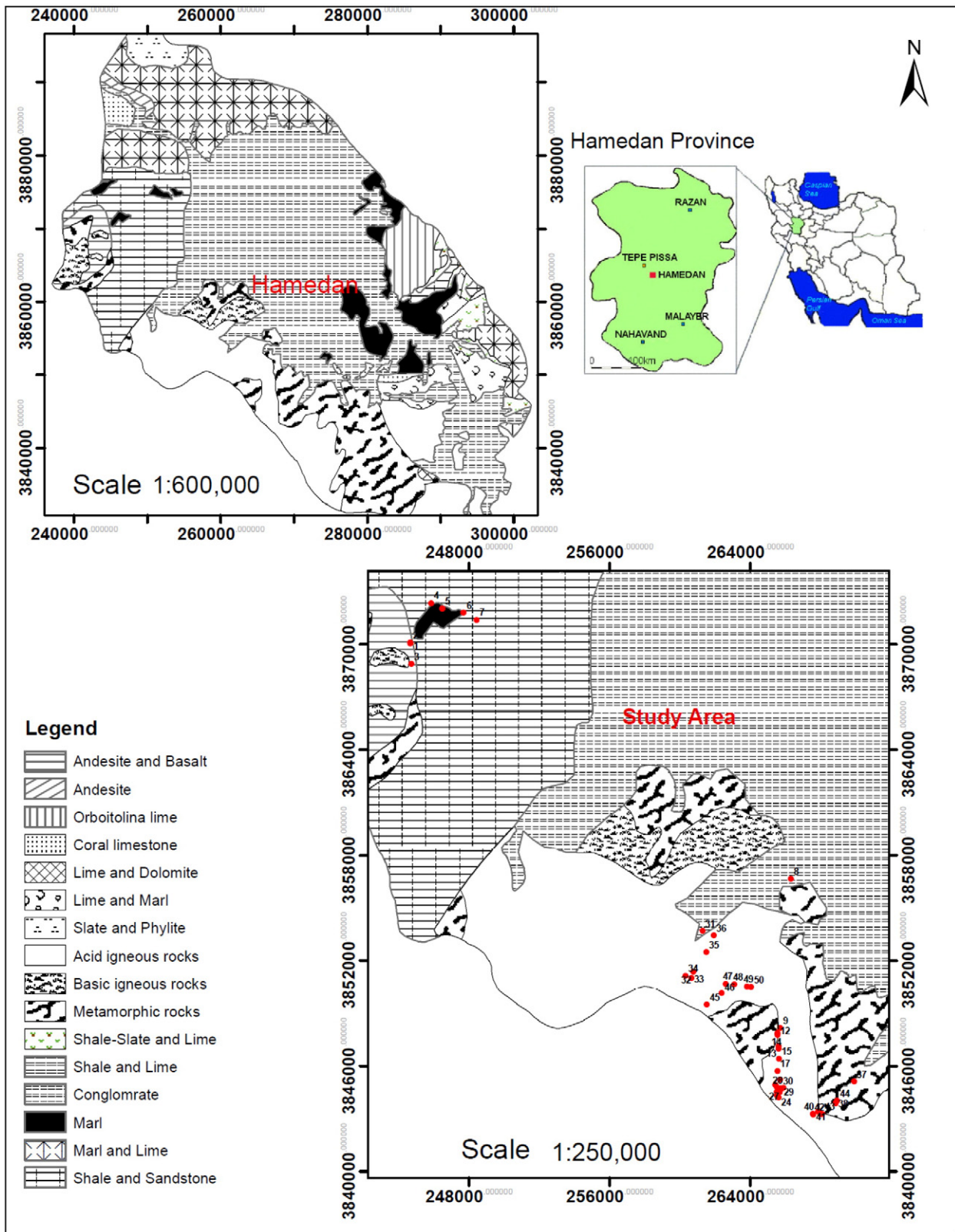


Fig. 1. Geological map of the studied area (Hamadan Regional Water Authority, HRWA) and location of spring water samples.

Thus, the objectives of this study were (1) to investigate chemical water compositions and the main geochemical reactions, which control the spring water composition in a high-mountain area

of Iran; (2) to define the background values of the cations and anions in spring waters; and (3) to evaluate the sites contaminated by trace elements.

**Table 1**  
Descriptive statistics of chemical compositions of spring water samples.

| Variable                                | Mean  | St dev | CV (%) | Minimum | Q1   | Median | Q3   | Maximum | Skewness |
|---|-------|--------|--------|---------|------|--------|------|---------|----------|
| pH                                      | 7.6   | 0.30   | 3.9    | 6.8     | 7.4  | 7.7    | 7.9  | 7.9     | -0.73    |
| Tem. (°C)                               | 14.3  | 3.03   | 21.2   | 9.0     | 12.0 | 14.0   | 16.0 | 21.9    | 0.68     |
| EC ( $\mu\text{S cm}^{-1}$ )            | 171   | 239    | 139.9  | 32      | 59   | 69     | 103  | 921     | 2.21     |
| TDS ( $\text{mg l}^{-1}$ )              | 117.7 | 163.3  | 138.7  | 20.7    | 35.6 | 45.2   | 83.2 | 589.4   | 2.08     |
| Cl ( $\text{mg l}^{-1}$ )               | 12.2  | 6.5    | 52.9   | 3.6     | 10.7 | 10.7   | 10.7 | 35.5    | 2.9      |
| HCO <sub>3</sub> ( $\text{mg l}^{-1}$ ) | 68.3  | 117.8  | 172.5  | 6.1     | 12.2 | 18.3   | 32.0 | 427.0   | 2.1      |
| SO <sub>4</sub> ( $\text{mg l}^{-1}$ )  | 14.4  | 15.0   | 103.8  | 2.0     | 4.8  | 10.5   | 14.2 | 69.9    | 2.5      |
| Ca ( $\text{mg l}^{-1}$ )               | 18.3  | 26.2   | 142.7  | 2.0     | 4.8  | 6.0    | 12.0 | 86.0    | 1.9      |
| Mg ( $\text{mg l}^{-1}$ )               | 5.5   | 6.9    | 126.0  | 1.2     | 2.4  | 3.3    | 4.2  | 28.8    | 2.5      |
| Na ( $\text{mg l}^{-1}$ )               | 5.9   | 7.5    | 128.4  | 2.0     | 2.7  | 3.3    | 4.5  | 36.8    | 3.1      |
| K ( $\text{mg l}^{-1}$ )                | 1.17  | 3.14   | 268.9  | 0.00    | 0.33 | 0.47   | 0.83 | 17.00   | 4.77     |
| P ( $\text{mg l}^{-1}$ )                | 0.30  | 0.20   | 68.09  | 0.06    | 0.21 | 0.26   | 0.31 | 1.39    | 3.78     |
| NO <sub>3</sub> ( $\text{mg l}^{-1}$ )  | 2.4   | 3.9    | 166.8  | 0.2     | 0.7  | 1.3    | 2.5  | 26.4    | 5.1      |
| Cd ( $\mu\text{g l}^{-1}$ )             | 125   | 45     | 35.9   | 50      | 84   | 127    | 59   | 208     | 0.000    |
| Fe ( $\mu\text{g l}^{-1}$ )             | 103   | 54     | 52.1   | 11      | 68   | 102    | 135  | 257     | 0.720    |
| Mn ( $\mu\text{g l}^{-1}$ )             | 128   | 51     | 39.5   | 22      | 92   | 137    | 165  | 227     | -0.420   |
| Ni ( $\mu\text{g l}^{-1}$ )             | 324   | 114    | 35.3   | 70      | 251  | 338    | 401  | 562     | -0.230   |
| Zn ( $\mu\text{g l}^{-1}$ )             | 50    | 36     | 71.9   | 32      | 39   | 46     | 49   | 293     | 6.650    |

## 2. Materials and methods

### 2.1. Study area and spring water sampling

Alvand (3580 m), one the most famous mountain of Iran is a sub range of the Zagros mountains in western Iran (Fig. 1), and lies between longitudes 47°14'28"E and latitudes 34°12'58"N. It placed 10 km south of the city of Hamedan in Hamedan Province (Fig. 1). Among the famous peaks of this range are Kalagh-Laneh and Daem-Barf and Ghezal-Arsalan.

The Alvand range is located in the Sanandaj-Sirjan geological and structural zone and are mainly consisted of intrusive rocks namely,

gabbros, granites, and leucocratic granitoids (Shahbazi et al., 2010). Mineral constituents of the gabbroic rocks are olivine, clinopyroxene, hornblende, biotite, plagioclase, and accessory mineral phases such as quartz, apatite, titanite, monazite, and zircon, while granites are mainly composed of orthoclase, plagioclase, microcline, quartz, and biotite, and accessory minerals include muscovite, tourmaline, apatite, titanite, zircon, and  $\pm$  chlorite (Shahbazi et al., 2010). Mineral constituents of the leucocratic granitoids are quartz, plagioclase, orthoclase, microcline, and accessory minerals including titanite, chlorite, muscovite, tourmaline, apatite, and zircon (Shahbazi et al., 2010). Geological map of the Alvand complex is shown in Fig. 1. Based on Aliani et al. (2012), the basement of the Alvand complex is composed of: (1) pre-Jurassic rocks consisting of schist, hornfels, phyllite, metasandstone, and metatuff units; (2) Jurassic rocks include shale, slate, marl, thin layers of limestone, sandstone, quartzite, and limestone; (3) Cretaceous sandstone, conglomerate, marly limestone, dolomitic limestone, and shale; (4) Oligo-Miocene basal conglomerate, marly limestone, marl, and limestone disconformably lay on the Cretaceous sediments or Jurassic slates. Altitudes of the site sampling ranged from about 1882 m to 3224 m above sea level.

The descriptive statistics of the soil properties of Alvand Mountain was determined by Jalali (2011) and following are some of the reported parameters by Jalali (2011):

The pH values of the soils averaged 6.4 and ranged from 5.0 to 7.4, the content of organic matter in the soils ranged between 0.45 and 8.0%, the content of clay-size particles ranges from 26 to 230  $\text{g kg}^{-1}$  with a mean value of 93  $\text{g kg}^{-1}$ . The range of EC, cation exchange capacity, and CaCO<sub>3</sub> equivalent was 0.051 to 0337  $\text{dS m}^{-1}$ , 1.3 to 6.6  $\text{cmol}_c \text{kg}^{-1}$ , and 0–8.4%, respectively.

The tribally organized groups carried out animal husbandry in the Alvand Mountain and the land serves as stubble pasture (Jalali, 2011). The dominant vegetation of this catchment consists of (Jalali, 2011): *As-tragalus spp.*, *Stipa barbata* Desf, *Euphorbia Aellenii* Rech. F., *Acantholimon Festucaaceum* Boiss., *Phlomis orientalis* Mill. Spring water samples in group 1 (Section 3.2) are located in the agricultural area, where crop production have been going on for about 30 years.

Water samples for chemical analysis were obtained during 2013 from the 50 spring waters shown in Fig. 1. Spring waters were sampled using acid washed polyethylene bottles. All water samples were stored in polyethylene bottles at 4 °C before further analysis. The water temperature, electrical conductivity (EC), and pH of the water samples were measured in the field during sampling using portable instruments (WTW, Germany), while calcium (Ca), magnesium (Mg), sodium (Na), potassium (K), bicarbonate (HCO<sub>3</sub>), sulphate (SO<sub>4</sub>) and chloride (Cl) were measured in the laboratory. In the laboratory, samples were analysed immediately for HCO<sub>3</sub> and Ca ions, while other determinations

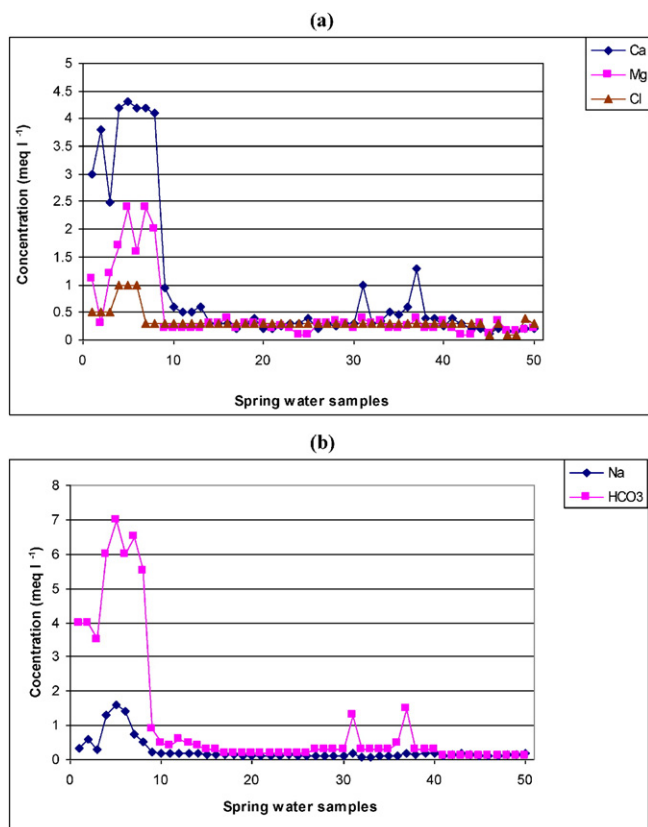


**Fig. 2.** Profile concentration of (a) Ca, Mg, and Cl and (b) Na and HCO<sub>3</sub> for spring water samples.

## Piper Diagram

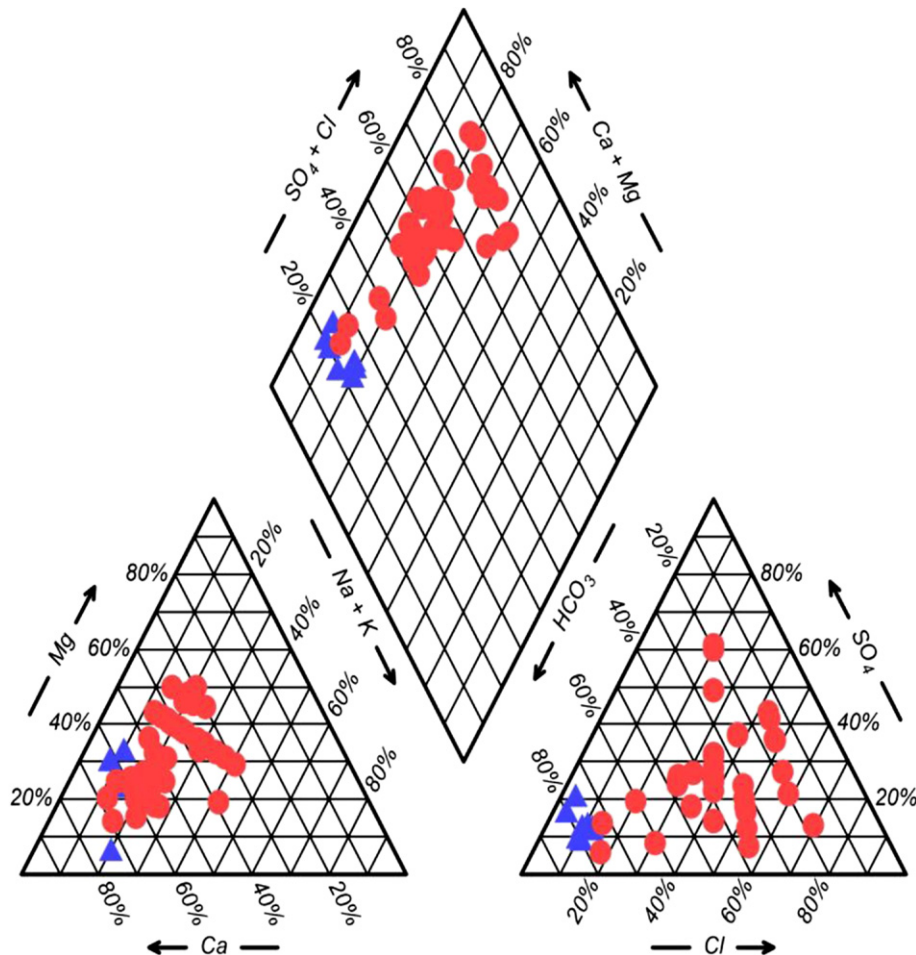


**Fig. 3.** Piper diagram indicates relative amounts of major ions analyzed in spring waters. Closed triangles indicate group 1 spring waters (high mineralization waters), while closed circles represent group 2 spring waters (low mineralization waters).

were made within 48 h after collection. Calcium, Mg, Cl, and  $\text{HCO}_3$  were determined by titration. Sodium and K were measured by flame photometry,  $\text{SO}_4$  by spectrophotometric turbidimetry and  $\text{NO}_3$  by colorimetry with an UV–visible spectrophotometer (Rowell, 1994). Phosphorous (P) was analyzed by the Murphey and Riley (1962) method. The trace elements concentration (Cd, Fe, Mn, Ni, Zn) in spring waters was determined by atomic absorption spectrometer. Aluminum and Si concentrations were not measured but as suggested by Gandois et al. (2010) their

activity were assessed by considering equilibrium of spring water samples with  $\text{SiO}_2$  and  $\text{Al}(\text{OH})_3$  using Visual Minteq program. A value of  $\log K_s = -4$  and 8.29 was selected for  $\text{SiO}_2$  and  $\text{Al}(\text{OH})_3$ , respectively. Ion speciation and mineral (e.g. calcite, dolomite) saturation indices were calculated in water samples using Visual Minteq program. Hardness is a measure of the combined concentrations of Ca and Mg in the water and following equation was used to define hardness as  $\text{mg l}^{-1}$  of calcium carbonate (Sawyer et al., 2003):

$$\text{TH} = (\text{as mg CaCO}_3 \text{ l}^{-1}) = (\text{Ca} + \text{Mg}) \text{ meq l}^{-1} \times 50.$$

Multivariate analysis was applied to the data to generate groups of correlated element and was used to predict processes occurring in the investigate environment. The statistical software package MINITAB (version 17.0, Minitab Inc.) was used for all calculations performed in this study.

### 2.2. Background value calculation

Statistical methods were made in spring waters in an effort to both establish background concentrations and identify possible contamination. In accordance with Tume et al. (2014), two methods were used in the evaluation of background values in spring waters. In the first method, the mean concentration and the standard deviation (SD)

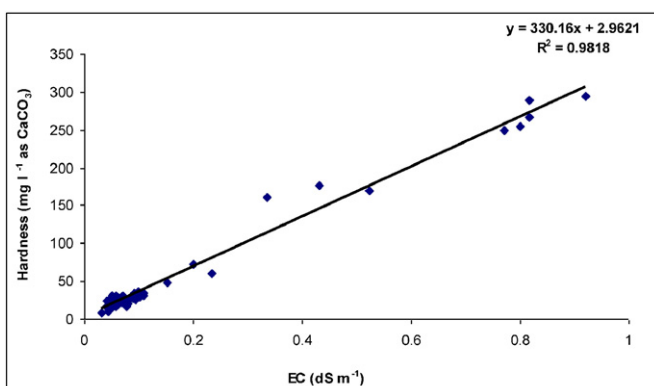


**Fig. 4.** Relation between hardness and electrical conductivity in spring water samples.

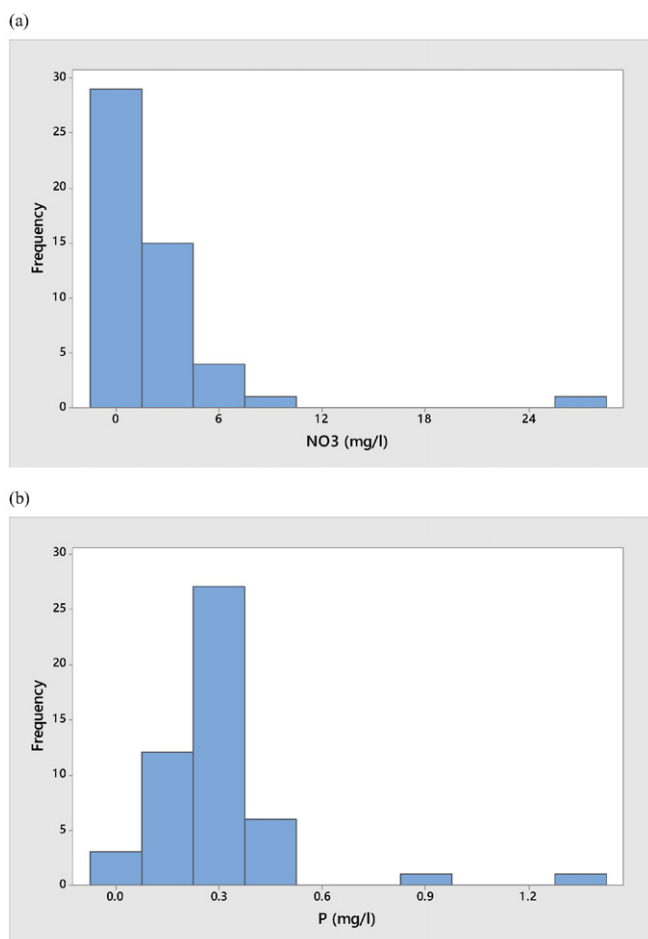


Fig. 5. Frequency of histogram of (a) NO<sub>3</sub> and (b) P in spring water samples.

were calculated using the mean + 2 × SD (Gil et al., 2004; Micó et al., 2006). In this method, the samples that were statistically identified as outliers (values > upper whisker), were removed and these samples were not used to establish background values in the study area. In the second method, the median ± 2MAD (median absolute deviation) was used to define the background values (Reimann et al., 2005). The upper whisker (= 3rd quartile + 1.5IQR (interquartile range)) was used as a limit to define the contamination in the spring waters (Tukey, 1977; Tume et al., 2014).

Table 2

Mean values of measured parameters in two groups of spring water samples.

| Group | pH               | Tem °C            | EC $\mu\text{S cm}^{-1}$ | Cl                | HCO <sub>3</sub>   | SO <sub>4</sub>   | Ca                | Mg $\text{mg l}^{-1}$ | Na                | K                | P                  | NO <sub>3</sub>  | Mn               | Cd               | Ni $\mu\text{g l}^{-1}$ | Zn              | Fe               |
|-------|------------------|-------------------|--------------------------|-------------------|--------------------|-------------------|-------------------|-----------------------|-------------------|------------------|--------------------|------------------|------------------|------------------|-------------------------|-----------------|------------------|
| 1     | 7.6 <sup>a</sup> | 16.6 <sup>a</sup> | 676.7 <sup>a</sup>       | 22.6 <sup>a</sup> | 324.1 <sup>a</sup> | 42.9 <sup>a</sup> | 75.7 <sup>a</sup> | 19.0 <sup>a</sup>     | 19.6 <sup>a</sup> | 4.7 <sup>a</sup> | 0.466 <sup>a</sup> | 7.3 <sup>a</sup> | 143 <sup>a</sup> | 137 <sup>a</sup> | 355 <sup>a</sup>        | 52 <sup>a</sup> | 115 <sup>a</sup> |
| 2     | 7.2 <sup>b</sup> | 13.8 <sup>b</sup> | 76.3 <sup>b</sup>        | 10.2 <sup>b</sup> | 19.6 <sup>b</sup>  | 9.0 <sup>b</sup>  | 7.4 <sup>b</sup>  | 2.9 <sup>b</sup>      | 3.2 <sup>b</sup>  | 0.5 <sup>b</sup> | 0.262 <sup>b</sup> | 1.4 <sup>b</sup> | 44 <sup>b</sup>  | 61 <sup>b</sup>  | 159 <sup>b</sup>        | 39 <sup>a</sup> | 41 <sup>b</sup>  |

Values that followed by the same letter within each column are not significantly different by Duncan's multiple range test ( $p \leq 0.05$ ).

Table 3

Comparison between mean values of major ion chemistry of two groups of spring water samples and groundwaters in the Bahar area (Jalali, 2005), near the studied area.

| Group             | pH  | EC $\mu\text{S cm}^{-1}$ | Cl   | HCO <sub>3</sub> | SO <sub>4</sub> $\text{mg l}^{-1}$ | NO <sub>3</sub> | Ca   | Mg   | Na   | K   |
|-------------------|-----|--------------------------|------|------------------|------------------------------------|-----------------|------|------|------|-----|
| 1                 | 7.6 | 676.7                    | 22.6 | 324.1            | 42.9                               | 7.3             | 75.7 | 19.0 | 19.6 | 4.7 |
| 2                 | 7.2 | 76.3                     | 10.2 | 19.6             | 9.0                                | 1.4             | 7.4  | 2.9  | 3.2  | 0.5 |
| Bahar groundwater | 7.8 | 834.5                    | 56.6 | 153.8            | 158.1                              | 41.2            | 73.4 | 36.8 | 43.8 | 2.5 |

Table 4

Average, minimum, and maximum values of saturation indices of common minerals for two groups of spring waters.

| Mineral  | Group 1 |       |       | Group 2 |       |       |
|--|---------|-------|-------|---------|-------|-------|
|  | Average | Min   | Max   | Average | Min   | Max   |
| Anhydrite  | -2.3    | -2.7  | -2.0  | -3.7    | -4.5  | -3.0  |
| Aragonite  | -0.2    | -0.8  | 0.1   | -2.0    | -3.6  | -0.9  |
| Calcite  | -0.1    | -0.7  | 0.2   | -1.9    | -3.4  | -0.8  |
| Dolomite (ordered)   | -0.6    | -1.8  | 0.1   | -4.0    | -7.0  | -2.1  |
| Gypsum   | -2.0    | -2.4  | -1.7  | -3.4    | -4.2  | -2.7  |
| Halite   | -8.0    | -8.4  | -7.4  | -9.0    | -9.5  | -8.8  |
| KCl(s)   | -8.6    | -9.5  | -7.6  | -9.5    | -11.6 | -9.0  |
| Lime   | -22.2   | -23.2 | -21.0 | -22.6   | -24.7 | -21.0 |
| Hydroxyapatite   | 4.8     | 1.7   | 6.8   | 2.1     | -5.0  | 4.5   |
| CaHPO <sub>4</sub> (s)   | -1.4    | -1.9  | -0.8  | -2.2    | -3.5  | -1.7  |
| Ca <sub>3</sub> (PO <sub>4</sub> ) <sub>2</sub> (beta)                 | -1.0    | -2.7  | 0.4   | -2.7    | -6.8  | -1.5  |
| Ca <sub>4</sub> H(PO <sub>4</sub> ) <sub>3</sub> :3H <sub>2</sub> O(s) | -3.6    | -6.0  | -1.9  | -6.4    | -12.2 | -4.3  |
| Otavite  | -0.1    | -0.4  | 0.2   | -0.4    | -1.2  | 0.2   |
| Ferrihydrite   | 3.2     | 2.6   | 3.7   | 4.0     | 3.4   | 4.7   |
| Goethite   | 6.1     | 5.6   | 6.6   | 7.0     | 6.4   | 7.6   |
| Hematite   | 14.6    | 13.5  | 15.6  | 16.4    | 15.2  | 17.6  |
| Rhodochrosite  | -1.0    | -1.4  | -0.7  | -1.1    | -2.0  | -0.5  |
| NiCO <sub>3</sub> (s)  | -0.5    | -1.3  | 0.0   | -0.8    | -1.8  | -0.1  |
| Ni(OH) <sub>2</sub>  | -2.2    | -3.2  | -1.3  | -0.8    | -1.7  | -0.1  |
| ZnCO <sub>3</sub> (s)  | -1.4    | -1.8  | -1.0  | -1.9    | -2.8  | -1.3  |
| Zn(OH) <sub>2</sub>  | -5.0    | -5.8  | -4.0  | -4.0    | -5.2  | -3.1  |

### 3. Results and discussion

#### 3.1. Major ion chemistry

Table 1 presents the descriptive statistical compositions of the spring water samples. The range of pH and EC was 6.8 to 7.9 and 32 to 921  $\mu\text{S cm}^{-1}$ , respectively. Water temperature in all samples averaged 14.3 °C and ranged from 9.0 to 21.9 °C. Fig. 2 indicates profiles concentration of Ca, Mg, Na HCO<sub>3</sub>, and Cl of all spring water samples. Among cations, Ca was generally the main cations representing on average (in meq l<sup>-1</sup>) 48.2% of all the cations, while Mg ions is secondary in importance, representing on average 31.4% of all cations. The bicarbonate is generally the main anion in spring waters representing on average 45.5% of all cations. Cl and SO<sub>4</sub> anions are secondary in importance, representing on average 34.4% and 23.1% of all anions, respectively. The CO<sub>2</sub> partial pressure (calculated by Phreeqc program) ranged between  $6.8 \times 10^{-5}$  to  $3.32 \times 10^{-2}$  atm. The mean CO<sub>2</sub> partial pressure ( $3.12 \times 10^{-3}$ ) is higher than the atmospheric value ( $3.47 \times 10^{-4}$  atm).

Piper diagram was used to determine type of the spring waters and hydrochemical facies (Fig. 3). The Piper diagram indicated that spring water samples belongs mainly to the Ca-HCO<sub>3</sub>, Ca-HCO<sub>3</sub>-Cl, CaMg-HCO<sub>3</sub>-Cl, and Ca-Mg-Cl-HCO<sub>3</sub>.

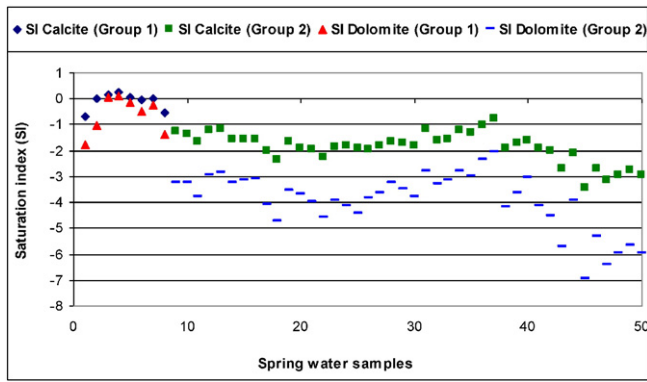


Fig. 6. Plots of saturation indices for calcite and dolomite for two groups of spring waters.

Hardness in all samples averaged  $60 \text{ mg l}^{-1}$  and ranged from 9 to  $294 \text{ mg l}^{-1}$ . Hardness is proportional to EC in most karstic waters (White, 2010) and strong correlation between these two parameters was obtained (Fig. 4). According to Sawyer et al. (2003) classification, the percentage of soft water ( $\text{TH} < 75.0 \text{ mg l}^{-1}$ ), and hard water ( $150\text{--}300 \text{ mg l}^{-1}$ ) in spring waters was 84% and 16%, respectively.

The Ca/Mg ratio varying from 0.5 to 12 and percentage of low Ca/Mg ratio ( $\leq 1.5$ ), and high Ca/Mg ratio ( $> 1.5$ ) in spring waters was 50%. Springs having dolomite minerals in the aquifer rock environment

have a Ca/Mg ratio near unity, while limestone springs have a Ca/Mg ratios in the range of 6–8 (White, 2010).

The quality of spring waters in Alvand Mountain was evaluated using recommended standards by World Health Organization (WHO, 2005). The data indicated that TH, Na, Cl, and  $\text{SO}_4$  in all spring water samples were lower than the highest limits of 450, 200, 250 and  $250 \text{ mg l}^{-1}$ , respectively, used for drinking purposed by WHO (2005).

Anions such as  $\text{NO}_3$  and P are major inorganic components deteriorating the quality of water for drinking purposes (Mehdi et al., 2015). Nitrate is the most common form of nitrogen that occurs in surface and groundwater and its concentrations are the result of different pollution processes, municipal wastewaters, fertilizers and manure application in agriculture. The frequency distribution chart (Fig. 5a) indicates that 72% of the samples contain  $\text{NO}_3$  in the range of  $0.21\text{--}2.0 \text{ mg l}^{-1}$  and that 32% of the samples contain less than  $1 \text{ mg NO}_3 \text{ l}^{-1}$ . Only one sample showed  $\text{NO}_3$  concentrations above the human affected value ( $13 \text{ mg l}^{-1}$   $\text{NO}_3$  is considered contaminated due to human activities) (Burkart and Kolpin, 1993; Eckhardt and Stackelberg, 1995). In Fig. 5b, the results of spring waters analysis for P concentration were shown as frequency distribution. The distribution of P concentration was positively skewed (3.78). Phosphorus concentrations in the spring waters varied from  $0.06$  to  $1.39 \text{ mg l}^{-1}$  with an average of  $0.30 \text{ mg l}^{-1}$ , and median value of  $0.26 \text{ mg l}^{-1}$ . The frequency distribution (Fig. 5b) indicated that 74% of the samples contained P in the range  $0.06\text{--}0.30 \text{ mg l}^{-1}$ , while only one sample contained more than  $1 \text{ mg l}^{-1}$ .

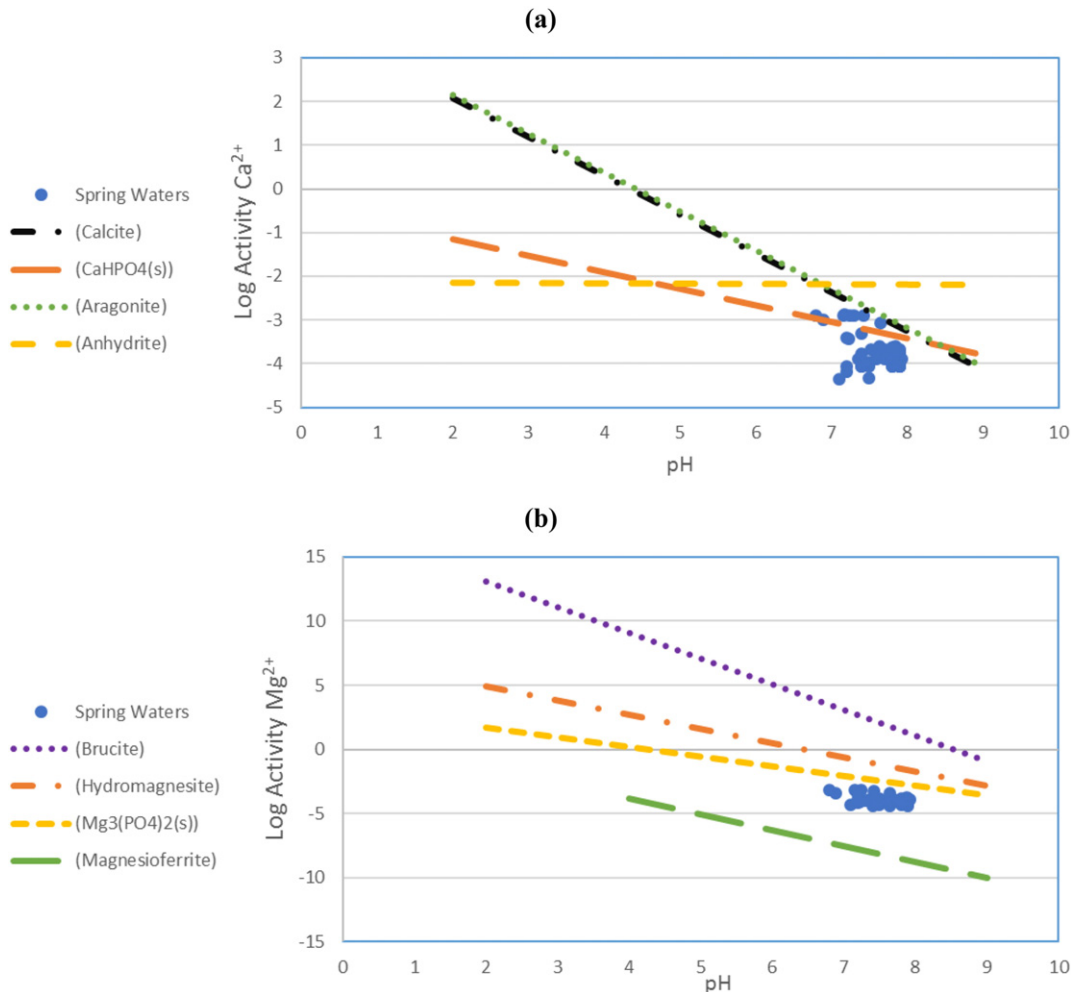


Fig. 7. The logarithm of Ca activities (a) and Mg activities (b) as a function of pH. The closed circle symbols represent spring water samples. The solid lines plot  $\text{Ca}^{2+}$  or  $\text{Mg}^{2+}$  activity constrained by different carbonate solubilities simulated using Visual Minteq program.

The descriptive statics for trace metals in spring waters was indicated in Table 1. The concentration of Cd, Fe, Mn, Ni, and Zn in spring waters averaged 125, 103, 128, 324 and 50  $\mu\text{g l}^{-1}$ , respectively. The desirable concentration of Fe in drinking water set by WHO (2011) is 300  $\mu\text{g l}^{-1}$ , and none of the spring water samples analyzed show above the limit. The WHO (2011) maximum admissible limit (MAL) for Cu and Mn are 2000 and 400  $\mu\text{g l}^{-1}$ , respectively and none of the

spring water samples analyzed show above the limit. No guideline is set by WHO (2011) for Zn level in drinking water, but none of the spring water samples analyzed show above the maximum admissible limit (5000  $\mu\text{g l}^{-1}$ ) set by USEPA (2012). Elevated Cd and Ni levels were observed in all spring water samples which are higher than the WHO (2011) MAL for Cd (3  $\mu\text{g l}^{-1}$ ) and Ni (70  $\mu\text{g l}^{-1}$ ) in drinking water samples. This may be mainly the consequence of the parent rock and the

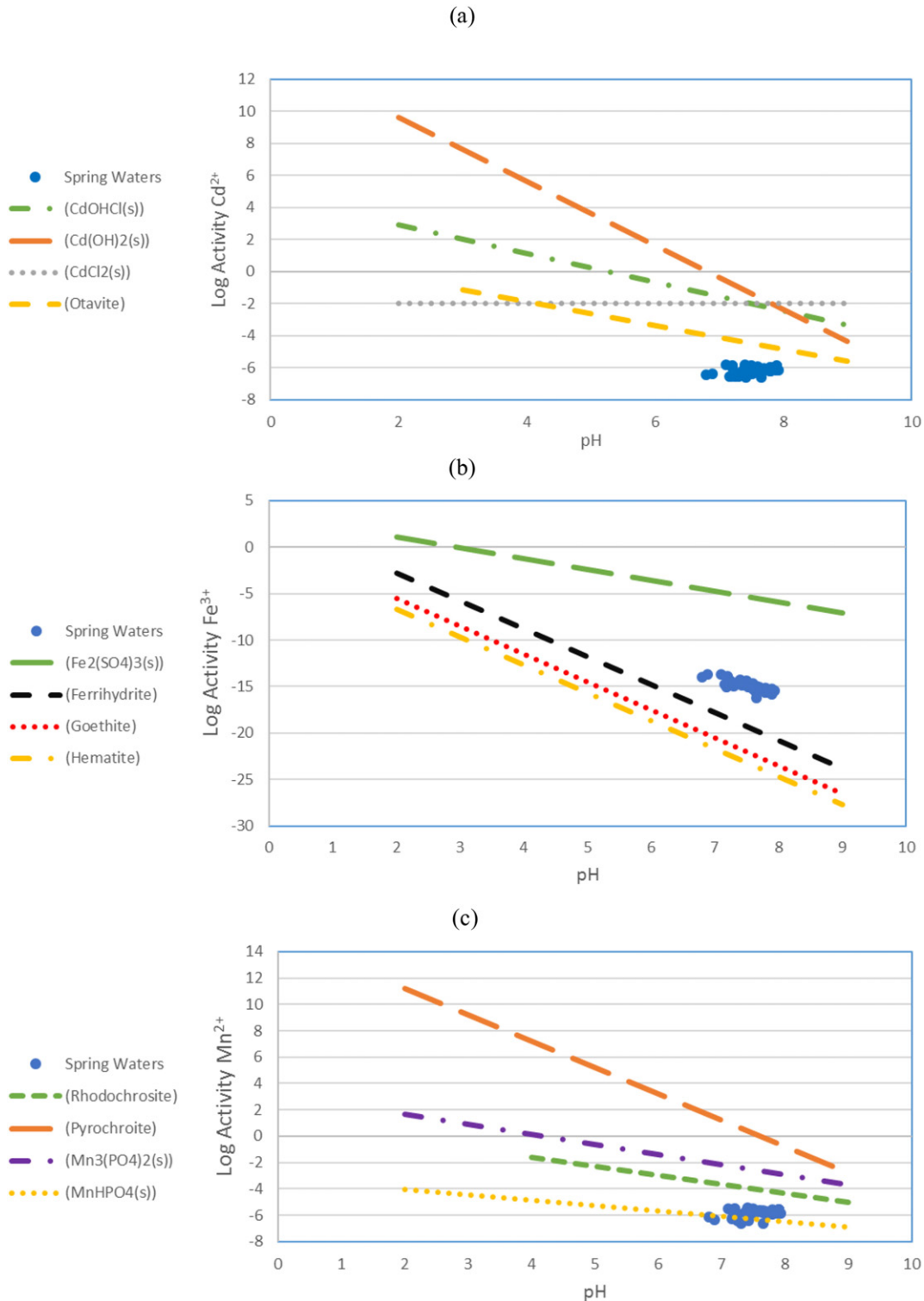


Fig. 8. The logarithm of (a)  $\text{Cd}^{2+}$ , (b)  $\text{Fe}^{3+}$ , (c)  $\text{Mn}^{2+}$ , (d)  $\text{Ni}^{2+}$ , and (e)  $\text{Zn}^{2+}$  activities as a function of pH. The closed circle symbols represent spring water samples. The solid lines plots  $\text{Cd}^{2+}$ ,  $\text{Fe}^{3+}$ ,  $\text{Mn}^{2+}$ ,  $\text{Ni}^{2+}$ , and  $\text{Zn}^{2+}$  activities constrained by different Cd, Fe, Mn, Ni, and Zn minerals solubility, respectively using Visual Minteq program.

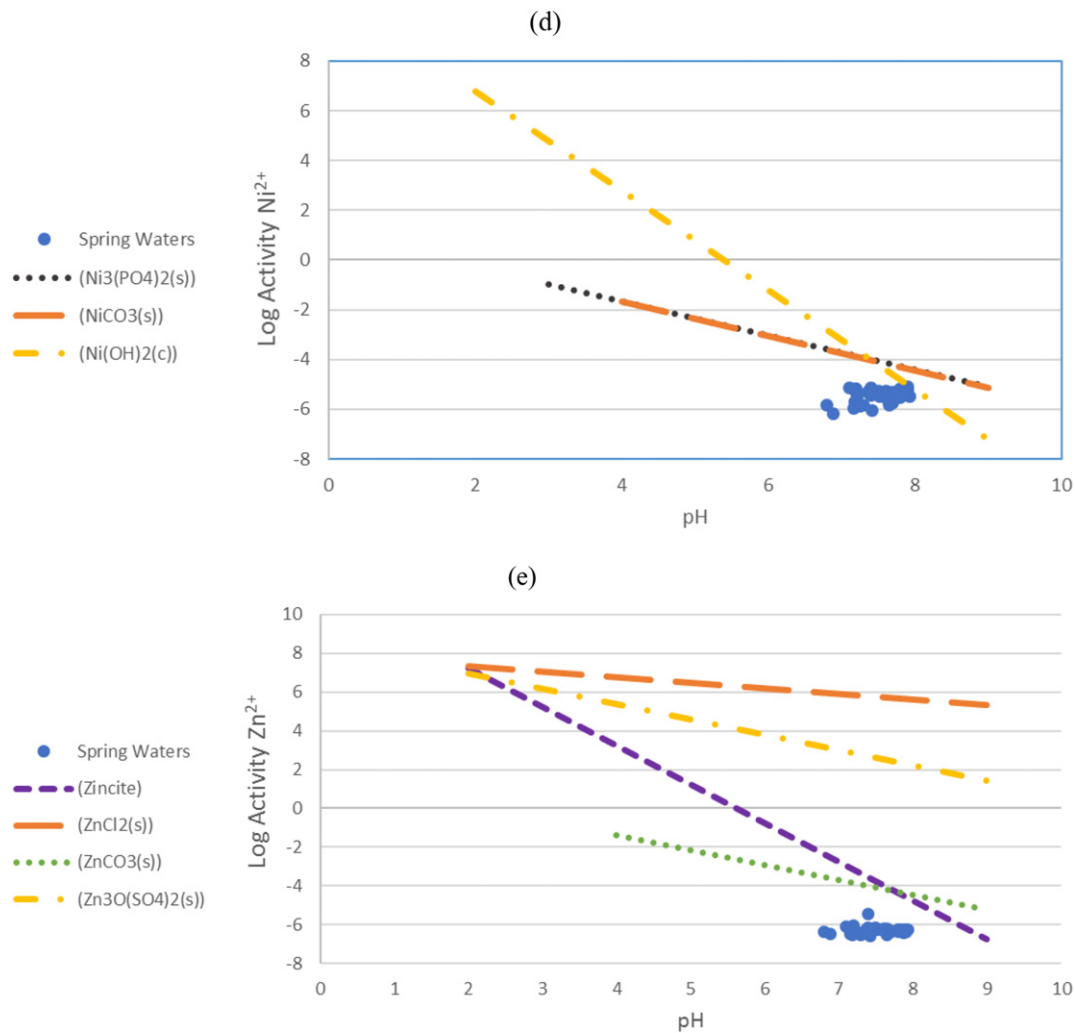


Fig. 8 (continued).

process of pedogenesis and partly reflecting an anthropogenic source from agricultural activities.

### 3.2. Water groups

In general according to the analytical data, all spring waters investigated can be classified into two groups 1: water types (Ca-HCO<sub>3</sub> 100%) and group 2: Ca-HCO<sub>3</sub>-Cl (19%), CaMg-HCO<sub>3</sub>-Cl (14.5), Ca-Mg-Cl-HCO<sub>3</sub> (12.5). Table 2 presents the mean values of ionic compositions for these two water groups. Differences between means values of two groups were analysed by analysis of variance (ANOVA) (Table 2). The Duncan's multiple range test was used to compare differences in means among two groups at the 0.05 probability level. The results indicated that all measured parameters (except Zn) were significantly different in two groups of spring water samples.

In Ca-HCO<sub>3</sub> water type, spring waters were relatively high in mineralization (average EC = 676.7  $\mu S\ cm^{-1}$ ) and was representative of 8 spring waters (16%). The EC varied from 335 to 921  $\mu S\ cm^{-1}$ , with low Cl and SO<sub>4</sub> content. Among the major cations, concentrations of Ca (in meq l<sup>-1</sup>) represented on average 61% of all the cations. Magnesium ions were secondary in importance, representing on average 24.4% of all cations. Among the major anions, HCO<sub>3</sub> generally dominates, representing on average 78% of all the anions. Cl and SO<sub>4</sub> ions were not abundant, they represented on average 12.6 and 9.4% of all the anions, respectively.

The second group comprised most spring waters (84%) of the studied area. In this group spring waters showed relatively lower EC, with values varying from 32.4 to 234.0  $\mu S\ cm^{-1}$  and the average value being 76.3  $\mu S\ cm^{-1}$ . The Ca/Mg ratio (average value 1.7) was less than group 1 (3.5). Calcium and Mg were dominant cation species, representing on average 46 and 33% of all the cations, respectively. Sodium was secondary in importance representing on average 20% of all cations. The concentrations of Cl and HCO<sub>3</sub> for this group of spring waters, representing on average 39% and 36% of all the anions. Sulfate ions was 25% of all anions. The weak salinity of these spring waters is thought to be linked either to an intrusive rock aquifer and a shorted time for weathering, and/or to the lack of sufficient amounts of soluble cation bearing minerals in the aquifer rock environment.

Some major ions were compared with those reported for ground waters located in the studied area (Jalali, 2005). He studied the ion chemistry in 135 ground water samples of the Bahar in Hamedan Province, Iran. The mean concentrations of HCO<sub>3</sub> and K found in spring water samples in group 1 (Table 3) were higher than those reported by Jalali (2005). Other parameters such as EC, Cl, Na, and Mg in both groups of spring water samples were lower than those reported for ground water samples. The mean NO<sub>3</sub> concentration in both spring water samples was lower than groundwater. Based on recommended standards by World Health Organization (WHO, 2005), the quality of spring waters in Alvand Mountain is higher than ground waters reported by Jalali



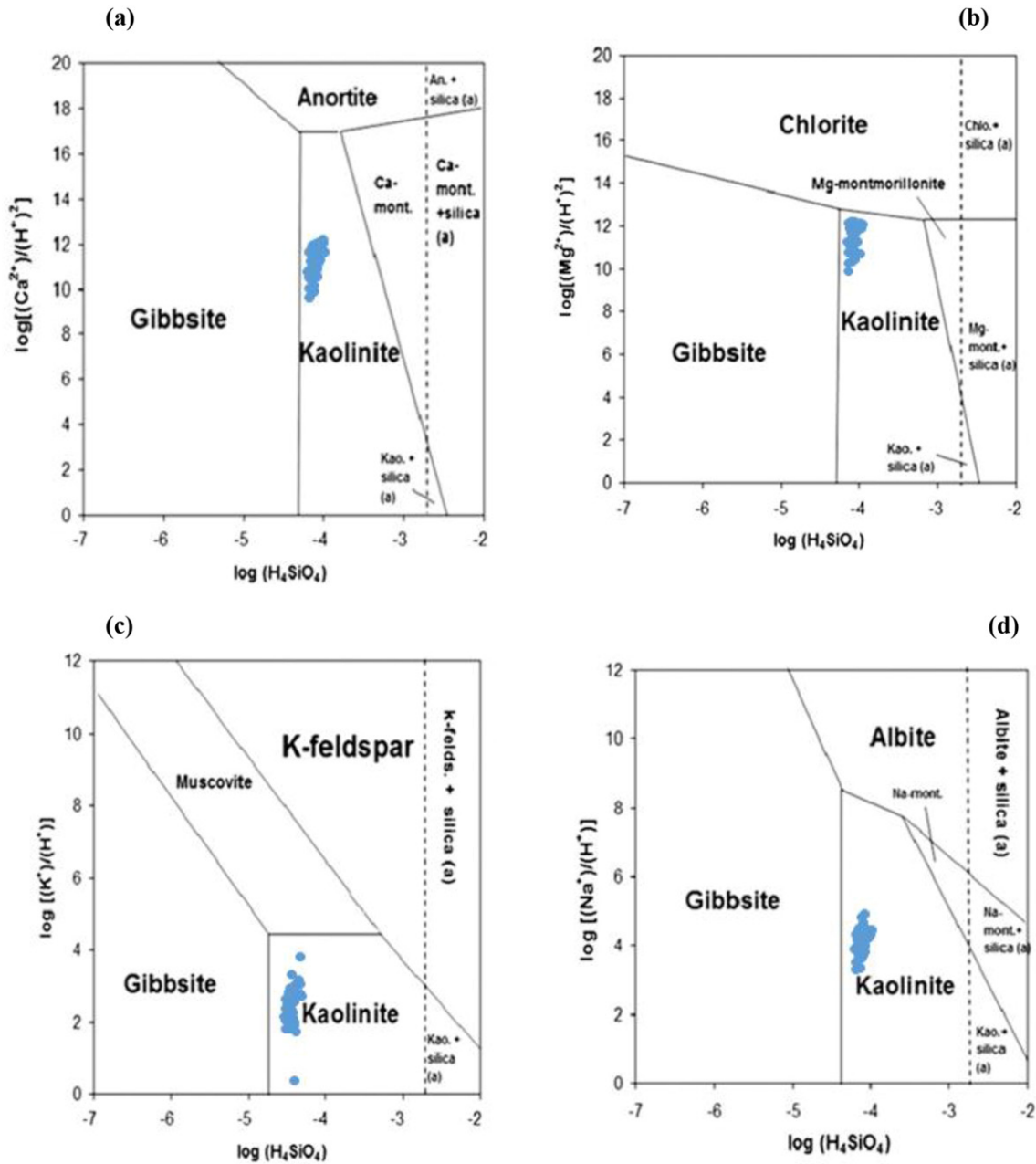


**Fig. 9.** Activity diagram of (a)  $\log [a_{Ca}/(a_H)^2]$  vs  $\log (H_4SiO_4)$ , (b)  $\log [a_{Mg}/(a_H)^2]$  vs  $\log (H_4SiO_4)$ , (c)  $\log (a_K/a_H)$  vs  $\log (H_4SiO_4)$ , (d)  $\log (a_{Na}/a_H)$  vs  $\log (H_4SiO_4)$  for silicate minerals, all at 15 °C and 1 bar (Marini et al., 2000). Circles represents spring water samples. The stability diagrams were taken from Marini et al. (2000).

(2005). This indicates that the spring water were less affected by anthropogenic activities.

### 3.3. Saturation index

Merkel and Planer-Friedrich (2002) indicated that equilibrium can be assumed for a range of  $-0.2$  to  $0.2$ . Saturation index values below  $-0.2$  indicates the solution is undersaturated for minerals and dissolution can be expected, while SI values higher than  $+0.2$ , indicates that the solution is supersaturated with a mineral and precipitation can be expected. Table 4 indicates SI of some common minerals in spring waters for two water groups calculated using Visual Mineq program. Spring water samples were under saturated with respect to dicalcium phosphate dehydrate ( $CaHPO_4 \cdot 2H_2O$ ), (average SI =  $-2.4$ ), dicalcium phosphate ( $CaHPO_4$ ) (average SI =  $-2.1$ ), octacalcium phosphate

( $Ca_8H_2(PO_4)_6 \cdot 5H_2O$ ), (average SI =  $-6.0$ ) beta-tricalcium phosphate [ $b-Ca_3(PO_4)_2$ ], (average SI =  $-2.4$ ) and supersaturated with respect to hydroxyapatites [ $Ca_5(PO_4)_3(OH)_2$ ] (average SI =  $2.5$ ). Most spring water samples were undersaturated with respect to calcite, as indicated by SI values (Table 4). The SI values of calcite ranged from  $-3.4$  to  $0.2$  with a mean of  $-1.59$ . Two water types differ from each other in their behaviour with respect to carbonate minerals. About 75% of spring waters in group 1 were at equilibrium with respect to calcite and dolomite (Fig. 6), suggesting that these carbonate mineral phases are present in the corresponding host rock. The geological map indicated that the original parent rock minerals in the studied area where spring waters of group 1 were sampled are mainly, made up of marl, shale and sandstone, andesite and basalt, and shale and lime (Fig. 1). In contrast, all spring waters in group 2 were under saturated with respect to calcite and dolomite, indicating that these carbonate mineral phases are not

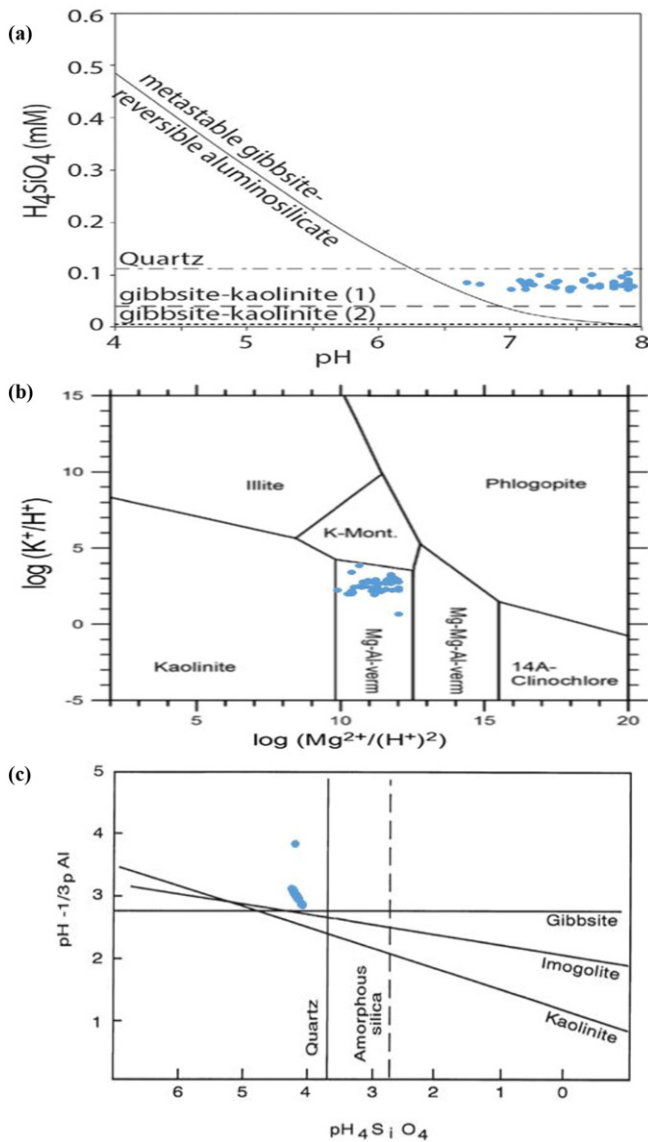


**Fig. 10.** (a) Relationship between pH and  $H_4SiO_4$  in spring waters. Equilibrium lines for aluminosilicate and secondary minerals are also indicated (the diagram was taken from Kim et al. (2014)). (b) Activity diagram of  $\log [K/(H)]$  vs  $\log(Mg/(H)^2)$  (the diagram was taken from Apollaro et al. (2013)). (c) Solubility diagram of  $pH - 1/3pAl$  vs  $pH_4SiO_4$  (the diagram was taken from Johnson and McBride (1991)). Circles represent spring water samples.

present in the host formation. Group 2 spring waters are probably linked to the circulation in non carbonate rocks such as intrusive rocks which were described in Section 2.1.

### 3.4. Solubility diagrams

Solubility diagrams have been shown to be useful for determining the solubility of interested minerals and also used as tools to suggest the possible presence of minerals in soil environments at various pH values. Any water sample plotted above or below mineral solubility line is supersaturated or undersaturated with respect to that particular mineral, respectively, while water sample plotted on or very near mineral solubility line is supposed to be at equilibrium with respect to that particular mineral. Fig. 7 indicates the logarithm of Ca activity ( $Ca^{2+}$ ) and Mg ( $Mg^{2+}$ ) as a function of pH, along with the solubility lines for

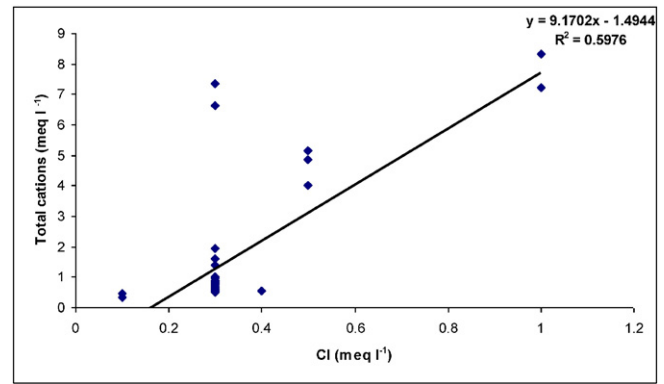


**Fig. 11.** Plot of total cations vs. Cl for spring water samples.

carbonate minerals. The spring water samples were mostly under saturated with respect to carbonate minerals.

Fig. 8 indicates the logarithm of Cd, Fe, Mn, Ni, and Zn activity as a function of pH, along with the solubility lines of minerals for above trace metals. The selected minerals were those that their activity values were within the activity values to the data. Fig. 8a present spring water Cd activities in relation to the stability of common Cd minerals. The Figure indicated that Cd in spring water samples were all undersaturated with respect to  $CdOHCl$ ,  $Cd(OH)_2$ ,  $CdCl_2$  and otavite. From this Figure and calculated SI (average SI =  $-0.35$ ) it may suggested that the solubility of Cd may be controlled by the solubility of the solid phase of otavite. Fig. 8b present spring water Fe activities in relation to the stability of common Fe minerals. Spring water samples were under saturated with respect to  $Fe_2(SO_4)_3$  and supersaturated with respect to ferrihydrate, goethite, and hematite (Fig. 8b). Fig. 8c present spring water Mn activities in relation to the stability of common Mnminerals. The Fig. 8c suggested that Mn in spring water samples were all supersaturated with respect to rhodochrosite,  $Mn_3(PO_4)_2$ , and pyrochroite, but were mostly in equilibrium with respect to  $MnHPO_4$  (average SI = 1.8), suggesting that the solubility of Mn may be controlled by the solubility of the solid phase of  $MnHPO_4$ . Fig. 8d presented spring water Ni activities in relation to the stability of common Ni minerals. Spring water samples were under saturated with respect to  $Ni_3(PO_4)_2$ ,  $NiCO_3$ , and  $Ni(OH)_2$ , but average value of SI for  $NiCO_3$  and  $Ni(OH)_2$  was  $-0.80$  and  $-1.0$ , respectively suggesting that these minerals may be controlled the solubility of Ni in studied spring waters. Fig. 8e presented spring water Zn activities in relation to the stability of common Zn minerals. The water samples were supersaturated by the  $ZnCl_2$ ,  $Zn_3O(SO_4)_2$ ,  $ZnCO_3$ , and zincite, while considering average value of SI for  $ZnCO_3$  ( $-1.8$ ) indicated that this mineral may control free Zn activity in spring water samples.

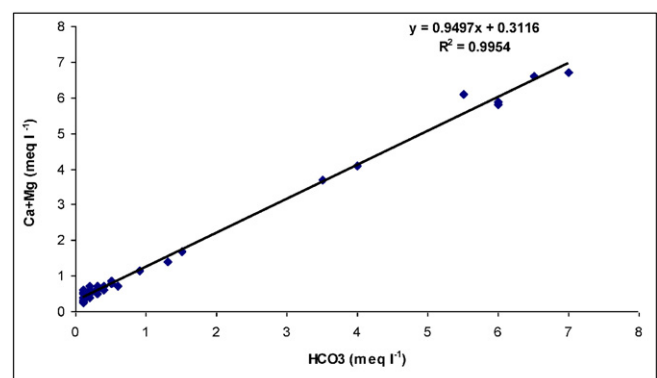


**Fig. 12.** Plot of Ca + Mg vs.  $HCO_3$  for spring water samples.

**Table 5**

Summary of the relationship between EC, pH, cations and anions in spring water samples.

|                  | pH       | EC       | Cl       | HCO <sub>3</sub> | SO <sub>4</sub> | Ca       | Mg       | Na       | K        | P      | NO <sub>3</sub> | Mn      | Cd      | Ni      | Zn    |
|------------------|----------|----------|----------|------------------|-----------------|----------|----------|----------|----------|--------|-----------------|---------|---------|---------|-------|
| EC               | -0.584** |          |          |                  |                 |          |          |          |          |        |                 |         |         |         |       |
| Cl               | -0.242   | 0.751**  |          |                  |                 |          |          |          |          |        |                 |         |         |         |       |
| HCO <sub>3</sub> | -0.575** | 0.992**  | 0.760**  |                  |                 |          |          |          |          |        |                 |         |         |         |       |
| SO <sub>4</sub>  | -0.582** | 0.932**  | 0.558**  | 0.908**          |                 |          |          |          |          |        |                 |         |         |         |       |
| Ca               | -0.584** | 0.983**  | 0.743**  | 0.990**          | 0.900**         |          |          |          |          |        |                 |         |         |         |       |
| Mg               | -0.498** | 0.940**  | 0.676**  | 0.944**          | 0.912**         | 0.898**  |          |          |          |        |                 |         |         |         |       |
| Na               | -0.443** | 0.905**  | 0.905**  | 0.897**          | 0.794**         | 0.869**  | 0.833**  |          |          |        |                 |         |         |         |       |
| K                | -0.358*  | 0.297    | 0.203    | 0.338*           | 0.184           | 0.427**  | 0.106    | 0.169    |          |        |                 |         |         |         |       |
| P                | -0.148   | 0.428**  | 0.547**  | 0.440*           | 0.319*          | 0.379*   | 0.480**  | 0.531**  | 0.066    |        |                 |         |         |         |       |
| NO <sub>3</sub>  | -0.544** | 0.626**  | 0.127    | 0.585**          | 0.717**         | 0.592**  | 0.639**  | 0.325*   | 0.143    | 0.062  |                 |         |         |         |       |
| Mn               | 0.253    | -0.670** | -0.559** | -0.701**         | -0.555**        | -0.716** | -0.610** | -0.578** | -0.413** | -0.180 | -0.307*         |         |         |         |       |
| Cd               | 0.165    | -0.597** | -0.516** | -0.620**         | -0.502**        | -0.631** | -0.556** | -0.519** | -0.290   | -0.108 | -0.261          | 0.944** |         |         |       |
| Ni               | 0.261    | -0.588** | -0.451** | -0.612**         | -0.508**        | -0.621** | -0.547** | -0.484** | -0.380*  | -0.206 | -0.314*         | 0.818** | 0.796** |         |       |
| Zn               | -0.125   | -0.118   | -0.035   | -0.132           | -0.114          | -0.139   | -0.110   | -0.089   | -0.093   | 0.364* | -0.048          | 0.386*  | 0.369*  | 0.287   |       |
| Fe               | 0.196    | -0.484** | -0.370*  | -0.504**         | -0.434**        | -0.524** | -0.455** | -0.370*  | -0.207   | -0.010 | -0.282          | 0.658** | 0.721** | 0.638** | 0.230 |

\* Correlations significant at p = 0.05.

\*\* Correlations significant at p = 0.01.

To obtain information on weathering of silicate minerals, ion activities calculated by Visual Minteq were plotted on activity diagrams for silicate minerals, at 15 °C and 1 bar (Marini et al., 2000). The activity plot of  $\log [aCa/(aH)^2]$  vs  $\log (H_4SiO_4)$  (Fig. 9a),  $\log [aMg/(aH)^2]$  vs  $\log (H_4SiO_4)$  (Fig. 9b),  $\log (aK/aH)$  vs  $\log (H_4SiO_4)$  (Fig. 9c),  $\log (aNi/aH)$  vs  $\log (H_4SiO_4)$  (Fig. 9d), for silicate minerals (Marini et al., 2000) indicated that most waters fall into the kaolinite field. Parisi et al. (2011) indicated that low residence time of water in the aquifer (such as most spring water samples in present study) would produce kaolinite only, while waters having enough residence time for interaction with aquifer, would produce both muscovite and smectite.

Fig. 10a indicated the relationship between pH and  $H_4SiO_4$  in spring waters along with equilibrium lines for aluminosilicate and secondary minerals. As it can be seen spring water samples fall into the gibbsite-kaolinite field. The activity plot of  $\log (K/H)$  vs  $\log [aMg/(aH)^2]$  (Fig. 10b), indicated that spring water samples fall into the K-Al-vermicolite field, suggesting that this mineral may partly control the K and Mg concentration. Fig. 10c showed the solubility diagram of pH-1/3pAl vs  $pH_4SiO_4$ , indicating that all water samples were saturated with respect to quartz, amorphous silica and gibbsite.

The source of CO<sub>2</sub> in spring water generally is soil gas, which has a PCO<sub>2</sub> of about  $3.45 \times 10^{-4}$  atm (Drever, 1988). The PCO<sub>2</sub> of the water samples ranged from  $6.8 \times 10^{-5}$  to  $3.32 \times 10^{-2}$  atm with a mean of  $3.12 \times 10^{-3}$ . The mean PCO<sub>2</sub> of group 1 ( $1.69 \times 10^{-2}$ ) was greater than group 2 ( $6.8 \times 10^{-4}$ ), indicating that CO<sub>2</sub> in group 1 is not limiting the dissolution of carbonate minerals throughout the aquifer. The high CO<sub>2</sub> in these spring water samples may be related to the agricultural

activities and production of CO<sub>2</sub> due to the degradation of organic matter and biological respiration (Minvielle et al., 2015). The low CO<sub>2</sub> in group 2 water samples may be related to both connection with aquifers with low CO<sub>2</sub> and dissolution of minerals such as Al-silicates which consumes CO<sub>2</sub> (Marini et al., 2000).

In addition to the low CO<sub>2</sub>, hydrogeological characteristics, and residence time of water in the aquifer may affected carbonate dissolution. Other processes involving cation exchange between spring waters and clay minerals may have influenced the observed chemical composition of these spring waters.

### 3.5. The origin of solutes

To identify the process that are responsible for generating the observed water compositions, computed pearson correlations coefficients was carried among dissolved species. The Cl and total cations (meq/l) relationship can be expected due to the dissolution of chloride salts or concentration processes by evaporation. The relationship between chloride and total cations shows most of the samples deviate from the 1:1 line (Fig. 11) ( $r^2 = 0.598$ ), indicating above processes are not the major source of total cations and Cl anion. The relation between Ca + Mg and HCO<sub>3</sub> was used to identify the impact of calcite and dolomite dissolution (Fig. 12). As indicated the concentrations of Ca and Mg are affected by the dissolution of carbonate minerals, such as dolomite and calcite. There was a strong positive correlation ( $r^2 = 0.995$ ) between these parameters indicating that calcite and dolomite dissolution contributes to Ca and Mg ions in these spring water samples. The presence of carbonate minerals in the soils of the studied area (Jalali, 2011), suggests that dissolution of these minerals will release significant amounts of Ca and Mg and HCO<sub>3</sub> to the spring waters. There was a high correlation coefficient ( $r = 0.905$ ) (Table 5) between Na and Cl, reflecting that halite may be a source of Na and Cl in spring waters. This mineral was not reported to be in the studied area. There was also relation between Na and SO<sub>4</sub> ( $r = 0.794$ ) (Table 5) indicating that the excess of sodium in these samples mostly resulted from the dissolution of sodium sulfate minerals. Possible role of silicate mineral dissolution and ion exchange in the chemistry composition of spring waters can be evaluated via plotting  $(Ca + Mg) - (HCO_3 + SO_4)$  in meq/l against  $(Na + K) - Cl$  meq l<sup>-1</sup> (Fig. 13). As suggested by some authors, if this water-rock interaction is significant in regulating water chemistry, the relation between these two parameters should be linear with a slope of -1.0 (Jalali, 2005, 2007; Kim et al., 2004). The correlation was significant ( $r^2 = 0.877$ ), but the slope was -1.803. Thus most of the spring water samples were not mainly influenced by silicate mineral dissolution and ion exchange.

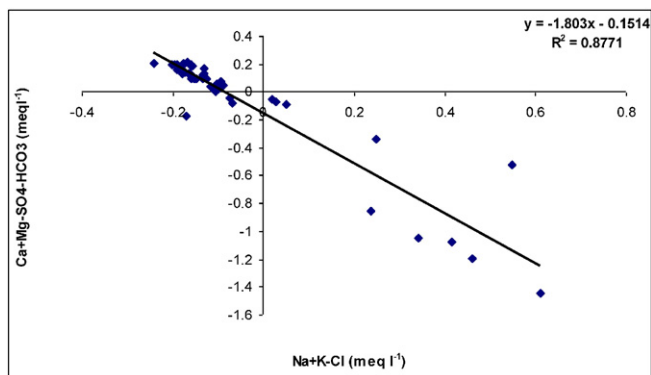


Fig. 13. Plot of Ca + Mg-SO<sub>4</sub>-HCO<sub>3</sub> vs. Na + K-Cl for spring water samples.

**Table 6**  
Unrotated factor loadings and communalities.

| Variable         | Factor 1 | Factor 2 | Factor 3 | Factor 4 | Factor 5 | Factor 6 | Factor 7 | Factor 8 | Factor 9 |
|------------------|----------|----------|----------|----------|----------|----------|----------|----------|----------|
| pH               | -0.553   | 0.329    | -0.511   | -0.302   | -0.013   | 0.252    | 0.39     | 0.098    | 0.077    |
| EC               | 0.972    | -0.177   | 0.054    | -0.066   | 0.072    | -0.019   | 0.046    | 0.025    | 0.017    |
| Cl               | 0.76     | -0.154   | -0.501   | 0.001    | 0.186    | -0.202   | 0.076    | 0.066    | 0.056    |
| HCO <sub>3</sub> | 0.978    | -0.141   | 0.022    | -0.023   | 0.08     | -0.015   | 0.041    | 0.005    | 0.001    |
| SO <sub>4</sub>  | 0.891    | -0.212   | 0.235    | -0.192   | 0.009    | 0.031    | 0.05     | 0.022    | 0.047    |
| Ca               | 0.974    | -0.093   | 0.067    | 0.051    | 0.099    | -0.04    | 0.097    | 0.033    | 0.014    |
| Mg               | 0.918    | -0.218   | 0.029    | -0.237   | -0.034   | 0.094    | 0.007    | -0.035   | -0.024   |
| Na               | 0.876    | -0.244   | -0.269   | -0.106   | 0.203    | -0.154   | -0.036   | 0.026    | 0.055    |
| K                | 0.364    | 0.215    | 0.166    | 0.812    | 0.272    | 0.091    | 0.22     | -0.034   | -0.001   |
| P                | 0.415    | -0.529   | -0.543   | 0.164    | -0.142   | 0.347    | -0.07    | -0.251   | -0.124   |
| NO <sub>3</sub>  | 0.581    | -0.187   | 0.646    | -0.168   | -0.183   | 0.255    | 0.157    | 0.042    | -0.019   |
| Mn               | -0.801   | -0.494   | 0.123    | -0.088   | 0.056    | -0.092   | 0.093    | -0.156   | 0.167    |
| Cd               | -0.739   | -0.558   | 0.156    | 0.009    | 0.174    | -0.014   | 0.079    | -0.18    | 0.172    |
| Ni               | -0.726   | -0.451   | 0.082    | -0.146   | 0.213    | -0.196   | 0.209    | 0.013    | -0.337   |
| Zn               | -0.185   | -0.664   | -0.129   | 0.356    | -0.547   | -0.131   | 0.079    | 0.236    | 0.039    |
| Fe               | -0.608   | -0.481   | 0.004    | 0.033    | 0.417    | 0.313    | -0.19    | 0.298    | 0.021    |
| Variance         | 8.8974   | 2.135    | 1.4512   | 1.0746   | 0.778    | 0.4963   | 0.3536   | 0.2855   | 0.2039   |
| %var             | 0.556    | 0.133    | 0.091    | 0.067    | 0.049    | 0.031    | 0.022    | 0.018    | 0.013    |

Dissolution of carbonate rocks produced Ca–HCO<sub>3</sub> or CaMg–HCO<sub>3</sub> water type throughout most of the aquifer. Thus, the primary geochemical process in the spring water samples in group 1 was carbonate-rock dissolution.

### 3.6. Factor analysis

Factor analysis was applied on the data of spring water samples in order to obtain more information about related parameters and to achieve the reduction of the variables. Table 6 shows the unrotated factor analysis, associated variance and communalities. Four factors had variance higher than one (the most significant one) (Miller and Miller, 2000). Two extracted factors explained 68.9% of data set variance. Factor 1 explained 55.6% of the total variance, while factor 2 explained 13.3%. Factor 1 had the highest (positive) factor loadings of EC, Cl, HCO<sub>3</sub>, SO<sub>4</sub>, Ca, Mg, Na, and negative factor loading of Mn, Cd, Ni, and Fe, and low factor loadings for the remaining parameters. These parameters have also correlated with each other (Table 5). This association strongly suggested that factor 1 may represent a parent rock variable, indicating of dissolution of calcite and dolomite and minerals containing trace metals. Factor 2 had the highest (negative) factor loadings of Zn and

can be considered as a lithogenic factor. Factor 3 explained 9.1% of the total variance and had the highest positive factor loading of NO<sub>3</sub> and negative factor loading of P. This factor may be named as anthropogenic factor. Factor 4 had the highest (positive) factor loadings of K and explained 6.7% of total variance and it can also be considered as lithogenic factor.

### 3.7. Background values and estimation of possible contamination

Anthropogenic influences lead to the enrichment of individual compartments or parts of natural systems. The background values for Cd, Fe, Mn, Ni, and Zn (calculated after the removal of values above the upper whisker following the mean + 2 × SD method) (BC1) were 214, 189, 229, 552, and 57 µg l<sup>-1</sup>, respectively. The background estimated with the median + 2 × MAD procedure (BC2) was indicated in Table 7. The background concentration in spring water samples estimated by the BC1 technique was higher than the BC2 (Table 7). The upper whisker values for Cd, Fe, Mn, Ni, and Zn were calculated as 272, 235, 275, 625, and 65 µg l<sup>-1</sup>, respectively. The concentration of Fe and Zn in 4% of water samples were higher than upper whisker values (Table 7), which may be related to the minerals of the igneous rocks in the studied

**Table 7**  
Descriptive statistics used to calculate background concentrations of measured parameters of spring water samples.

| Variable                               | Mean   | SD     | Median | MAD    | Q3     | IQR  | Whisker value | BC1 <sup>a</sup> | BC2 <sup>b</sup> | Outlier | Percentage of outlier samples |
|--|--------|--------|--------|--------|--------|------|---------------|------------------|------------------|---------|-------------------------------|
| EC (µS cm <sup>-1</sup> )              | 172.4  | 239.5  | 70     | 22.3   | 107.8  | 51.2 | 184.6         | 155.8            | 114.6            | 8       | 16                            |
| Cl (mg l <sup>-1</sup> )               | 12.212 | 6.461  | 10.65  | 0      | 10.65  | 0.0  | 10.7          | 13.8             | 10.7             | 7       | 14                            |
| HCO <sub>3</sub> (mg l <sup>-1</sup> ) | 68.3   | 117.8  | 18.3   | 9.1    | 32     | 19.8 | 61.7          | 55.3             | 36.7             | 8       | 16                            |
| SO <sub>4</sub> (mg l <sup>-1</sup> )  | 14.41  | 14.95  | 10.47  | 4.24   | 14.2   | 9.4  | 28.3          | 18.5             | 19.0             | 6       | 12                            |
| Ca (mg l <sup>-1</sup> )               | 18.34  | 26.18  | 6      | 2      | 12     | 7.3  | 22.9          | 14.6             | 10.0             | 9       | 18                            |
| Mg (mg l <sup>-1</sup> )               | 5.455  | 6.875  | 3.3    | 0.9    | 4.2    | 1.8  | 6.9           | 5.0              | 5.1              | 7       | 14                            |
| Na (mg l <sup>-1</sup> )               | 5.87   | 7.54   | 3.29   | 0.73   | 4.54   | 1.8  | 7.3           | 5.3              | 4.8              | 7       | 14                            |
| K (mg l <sup>-1</sup> )                | 1.166  | 3.135  | 0.472  | 0.218  | 0.83   | 0.5  | 1.6           | 1.1              | 0.9              | 3       | 6                             |
| P (mg l <sup>-1</sup> )                | 0.2955 | 0.2012 | 0.2564 | 0.0428 | 0.3114 | 0.10 | 0.46          | 0.40             | 0.34             | 5       | 10                            |
| NO <sub>3</sub> (mg l <sup>-1</sup> )  | 2.353  | 3.924  | 1.314  | 0.655  | 2.477  | 1.7  | 5.1           | 3.4              | 2.6              | 5       | 10                            |
| Cd (µg l <sup>-1</sup> )               | 124.7  | 448.4  | 126.5  | 365    | 159.3  | 75   | 272           | 214              | 200              | 0       | 0                             |
| Fe (µg l <sup>-1</sup> )               | 103.0  | 53.8   | 101.5  | 31     | 134.7  | 67   | 235           | 189              | 164              | 2       | 4                             |
| Mn (µg l <sup>-1</sup> )               | 127.9  | 50.6   | 137.0  | 335    | 165.5  | 73   | 275           | 229              | 204              | 0       | 0                             |
| Ni (µg l <sup>-1</sup> )               | 323.6  | 114.1  | 337.5  | 77     | 400.5  | 150  | 625           | 552              | 492              | 0       | 0                             |
| Zn (µg l <sup>-1</sup> )               | 49.7   | 35.7   | 45.5   | 5.3    | 49.4   | 10   | 65            | 57               | 56               | 2       | 4                             |

Method 1 = mean + 2 × SD (after removal outlier values).

Method 2 = median ± 2MAD (median absolute deviation).

Upper whisker (= 3rd quartile + 1.5 IQR (interquartile range)).

<sup>a</sup> Background concentration using method 1.

<sup>b</sup> Background concentration using method 2.

area. The background values for P and NO<sub>3</sub> (method 1) were 0.4 and 3.4 mg l<sup>-1</sup>, respectively. Of 50 spring water samples 5 (10%) and 8 (16%) samples had levels in excess of the background values for P and NO<sub>3</sub> (Table 7). In general, the mean concentration of measured parameters in group 1 water samples were higher than group 2. One reason might be that the in the studied area where spring waters of group 1 were sampled, anthropogenic sources such as agriculture activities, including wheat production, have been going on for about 30 years.

#### 4. Conclusions

The present work was designed to obtain for the first time knowledge on the chemistry and background values of cations and anions and some trace elements in spring waters of the Hamedan, western Iran. The chemical compositions indicated that the spring waters can be grouped into the two types of water. The first group characterized by relatively high TDS and high ion concentrations, while spring water samples included in group 2 were distinguished by very low mineralization and mean concentration of ions. The springs waters chemistry was mainly related to water–rock interaction processes. Four factors described the main processes affecting spring water chemistry: factor 1 marked by strong correlation of EC, Cl, HCO<sub>3</sub>, SO<sub>4</sub>, Ca, Mg, Na, Mn, Cd, Ni, and Fe. The second and third factors marked by high loading of Zn and NO<sub>3</sub>, P, respectively. Factor 4 had high factor loading of K. Factors 1, 2 and 4 together may be reflects natural hydrogeochemical processes, connected mainly with the dissolution of calcite, dolomite (group 1) and silicate weathering, while factor 3 may be resulted from anthropogenic input. The geochemical background values for measured parameters were determined using basic descriptive statistics. The spring water samples were mostly under saturated with respect to carbonate minerals and activity diagrams showed that spring waters fall into the kaolinite field. Our results indicated that trace metal concentrations and major ion chemistry in spring water samples were mainly the consequence of the parent rock and the process of pedogenesis and that only small number of spring waters showed degree of pollution of NO<sub>3</sub> and P.

#### Acknowledgments

We thank two reviewers for their useful comments that improved the quality of manuscript.

#### References

- Aliani, F., Maanijou, M., Sabouri, Z., Sepahi, A.A., 2012. Petrology, geochemistry and geotectonic environment of the Alvand Intrusive Complex, Hamedan, Iran. *Chem Erde* 72, 363–383.
- Allan, J.D., Flecker, A.S., 1993. Biodiversity conservation in running waters. *Bioscience* 43, 32–43.
- Apollaro, C., Marini, L., Critelli, T., De Rosa, R., 2013. The standard thermodynamic properties of vermiculites and prediction of their occurrence during water–rock interaction. *Appl. Geochem.* 35, 264–278.
- Bottoni, P., Óvári, M., Zárny, G., Caroli, S., 2013. Characteristics of spring waters in Budapest: a short review. *Microchem. J.* 110, 770–774.
- Boy-Roura, M., Menció, A., Mas-Pla, J., 2013. Temporal analysis of spring water data to assess nitrate inputs to groundwater in an agricultural area (Osona, NE Spain). *Sci. Total Environ.* 452–453, 433–445.
- Bozau, E., Stárk, H., Strauch, G., 2013. Hydrogeochemical characteristics of spring water in the Harz Mountains, Germany. *Chem. Erde* 73, 283–292.
- Burkart, M.R., Kolpin, D.W., 1993. Hydrologic and land use factors associated with herbicides and nitrates in near-surface aquifers. *J. Environ. Qual.* 22, 646–656.
- Drever, J.L., 1988. *The Geochemistry of Natural Waters*. second ed. Prentice Hall, Englewood Cliffs.
- Eckhardt, D.A.V., Stackelberg, P.E., 1995. Relation of groundwater quality to land use on Long Island, New York. *Ground Water* 33, 1019–1033.
- Gandois, L., Probst, A., Dumata, C., 2010. Modelling trace metal extractability and solubility in French forest soils by using soil properties. *Eur. J. Soil Sci.* 61, 271–286.
- Gil, C., Boluda, R., Ramos, J., 2004. Determination and evaluation of cadmium lead and nickel in greenhouse soils of Almería (Spain). *Chemosphere* 55, 1027–1034.
- Grasby, S.E., Hutcheon, I., 2000. Chemical dynamics and weathering rates of a carbonate basin Bow River, Southern Alberta. *Appl. Geochem.* 15, 67–77.
- Jalali, M., 2005. Major ion chemistry in the Bahar area, Hamadan, Western Iran. *Environ. Geol.* 47, 763–772.
- Jalali, M., 2007. Assessment of the chemical components of Famenin groundwater, Western Iran. *Environ. Geochem. Health* 29, 357–374.
- Jalali, M., 2011. Major ion chemistry of soil solution of mountainous soils, Alvand, Hamadan, Western Iran. *Soil Sediment Contam.* 20, 493–508.
- Johnson, M.J., McBride, M.B., 1991. Solubility of aluminum and silicon in acidified spodosols: evidence for soluble aluminosilicate. In: Wright, R.J., et al. (Eds.), *Plant–Soil Interactions at Low pH*. Kluwer Academic Publishers, PLSO AS02, pp. 15–24.
- Karimi, H., Raeisi, E., Bakalowicz, M., 2005. Characterizing the main karst aquifers of the Alvand basin, northwest of Zagros, Iran, by a hydrochemical approach. *Hydrogeol. J.* 13, 787–799.
- Kim, K., Rajmohan, N., Kim, H.J., Hwang, G.S., Cho, M.J., 2004. Assessment of groundwater chemistry in a coastal region (Kunsan, Korea) having complex contaminant sources: a stoichiometric approach. *Environ. Geol.* 46, 763–774.
- Kim, H., Bishop, J.K.B., Dietrich, W.E., Fung, I.Y., 2014. Process dominance shift in solute chemistry as revealed by long-term high-frequency water chemistry observations of groundwater flowing through weathered argillite underlying a steep forested hill-slope. *Geochim. Cosmochim. Acta* 140, 1–19.
- Lourenço, C., Ribeiro, L., Cruz, J., 2010. Classification of natural mineral and spring bottled waters of Portugal using principal component analysis. *J. Geochem. Explor.* 107, 362–372.
- Margiotta, S., Mongelli, G., Summa, V., Paternoster, M., Fiore, S., 2012. Trace element distribution and Cr(VI) speciation in Ca–HCO<sub>3</sub> and Mg–HCO<sub>3</sub> spring waters from the northern sector of the Pollino massif, Southern Italy. *J. Geochem. Explor.* 115, 1–12.
- Marini, L., Ottonello, G., Canepa, M., Cipolli, F., 2000. Water–rock interaction in the Bisagno valley (Genoa, Italy): application of an inverse approach to model spring water chemistry. *Geochim. Cosmochim. Acta* 64, 2617–2635.
- Matić, N., Miklavčić, I., Maldini, K., Tomas, D., Cuculić, V., Cardellini, C., Frančišković-Bilinski, S., 2013. Geochemical and isotopic characteristics of karstic springs in coastal mountains (Southern Croatia). *J. Geochem. Explor.* 132, 90–110.
- Mehdi, B., Ludwig, L., Lehner, B., 2015. Evaluating the impacts of climate change and crop land use change on streamflow, nitrates and phosphorus: A modeling study in Bavaria. *J. Hydrol. Regional Studies Part B* 60–90.
- Merkel, B.J., Planer-Friedrich, B., 2002. In: Nordstrom, D.K. (Ed.), *Ground-Water Geochemistry: A Practical Guide to Modeling of Natural and Contaminated Aquatic Systems*. Springer-Verlag, Berlin Heidelberg.
- Micó, C., Recatalá, L., Peris, M., Sánchez, J., 2006. Assessing heavy metal sources in agricultural soils of an European Mediterranean area by multivariate analysis. *Chemosphere* 65, 863–872.
- Miller, N.J., Miller, J.C., 2000. *Statistics and Chemometrics for Analytical Chemistry*. fourth ed. Pearson Education, Englewood Cliffs, NJ.
- Miller, B.V., Lerch, R.N., Groves, Ch.G., Polk, J.S., 2015. Recharge mixing in a complex tributary spring system in the Missouri Ozarks, USA. *Hydrogeol. J.* 23, 451–465.
- Minvielle, S., Lastennet, R., Denis, A., Peyraube, N., 2015. Characterization of karst systems using Sic–Pco<sub>2</sub> method coupled with PCA and frequency distribution analysis. Application to karst systems in the Vaucluse county (Southeastern France). *Environ. Earth Sci.* 74, 7593–7604.
- Murphy, J., Riley, J.P., 1962. A modified single solution method for the determination of phosphate in natural waters. *Anal. Chim. Acta* 27, 31–36.
- Nisi, B., Vaselli, O., Tassi, F., Elio, J., Huertas, A., Mazadiego, L., Ortega, M., 2013. Hydrogeochemistry of surface and spring waters in the surroundings of the CO<sub>2</sub> injection site at Hontomin–Huermeces (Burgos, Spain). *Int. J. Greenh. Gas Control* 14, 151–168.
- Parisi, S., Paternoster, M., Perri, F., Mongelli, G., 2011. Source and mobility of minor and trace elements in a volcanic aquifer system: Mt. Vulture (Southern Italy). *J. Geochem. Explor.* 110, 233–244.
- Ragno, G., De Luca, M., Ioele, G., 2007. An application of cluster analysis and multivariate classification methods to spring water monitoring data. *Microchem. J.* 87, 119–127.
- Reimann, C., Filzmoser, P., Garrett, R.G., 2005. Background and threshold: critical comparison of methods of determination. *Sci. Total Environ.* 346, 1–16.
- Rowell, D.L., 1994. *Soil Science: Methods and Applications*. Longman Scientific and Technical.
- Sawyer, N.N., McCarty, P.L., Parkin, G.F., 2003. *Chemistry for Environmental Engineering and Science*. fifth ed. McGraw-Hill, New York (752 pp.).
- Shahbazi, H., Siebel, W., Pourmoafae, M., Ghorbani, M., Sepahi, A.A., Shang, C.K., Vousoughi Abedini, M., 2010. Geochemistry and U–Pb zircon geochronology of the Alvand plutonic complex in Sanandaj–Sirjan Zone (Iran): new evidence for Jurassic magmatism. *J. Asian Earth Sci.* 39, 668–683.
- Tukey, J.W., 1977. *Exploratory Data Analysis*. Addison-Wesley, Reading.
- Tume, P., King, R., González, E., Bustamante, G., Reverter, F., Roca, N., Bech, J., 2014. Trace element concentrations in schoolyard soils from the port city of Talcahuano, Chile. *J. Geochem. Explor.* 147 (Part B), 229–236.
- USEPA (US Environmental Protection Agency), 2012. *Ground Water and Drinking Water*. <http://www.water.epa.gov/drink/index.cfm>.
- White, W.B., 2010. Springwater geochemistry. In: Kresic, N., Stevanovic, Z. (Eds.), *Ground-water Hydrology of Springs*. Engineering, Theory, Management, and Sustainability, P.241. 30 Corporate Drive, Suite 400, Burlington, MA 01803, USA Linacre House, Jordan Hill, Oxford OX2 8DP, UK.
- WHO (World Health Organization), 2005. *Guidelines for Drinking-water Quality*. third ed. (Geneva).
- WHO (World Health Organization), 2011. *Guidelines for Drinking-water Quality*. fourth ed. ([http://www.who.int/publications/2011/9789241548151\\_eng.pdf](http://www.who.int/publications/2011/9789241548151_eng.pdf)).
- Zelazny, M., Astel, A., Wolanin, A., Malek, 2011. Spatiotemporal dynamics of spring and stream water chemistry in a high-mountain area. *Environ. Pollut.* 159, 1048–1057.
- Zhang, Q., Zheng, Q., Sun, G., 2011. Arsenic-contaminated cold-spring water in mountainous areas of Hui County, Northwest China: a new source of arsenic exposure. *Sci. Total Environ.* 409, 5513–5516.